



1 **Turbulence and hypoxia contribute to dense zooplankton**
2 **scattering layers in Patagonian Fjord System.**

3 **Authors:** Iván Pérez-Santos^{1-2*}, Leonardo Castro²⁻³, Nicolás Mayorga¹, Lauren Ross⁴, Luis
4 Cubillos²⁻³, Mariano Gutierrez⁵, Edwin Niklitschek¹, Eduardo Escalona², Nicolás Alegría⁶ and
5 Giovanni Daneri²⁻⁷.

6 ¹Centro i~mar, Universidad de Los Lagos, Puerto Montt, Chile.

7 ²COPAS Sur-Austral, Universidad de Concepción, Campus Concepción, Víctor Lamas 1290,
8 Casilla 160-C, código postal: 4070043, Concepción, Chile.

9 ³Departamento de Oceanografía, Universidad de Concepción, Campus Concepción, Víctor
10 Lamas 1290, Casilla 160-C, código postal: 4070043, Concepción, Chile.

11 ⁴Department of Civil and Environmental Engineering, University of Maine, 5711 Boardman
12 Hall, Orono, ME 04469-5711.

13 ⁵Universidad Nacional Federico Villareal, Facultad de Oceanografía, Pesquerías y Ciencias
14 Alimentarias, Calle Francia 726, Miraflores, Lima, Perú.

15 ⁶Instituto de Investigaciones Pesqueras, Talcahuano, Chile.

16 ⁷Centro de Investigaciones en Ecosistemas de la Patagonia (CIEP), Coyhaique, Chile.

17 ***Corresponding author:** Iván Pérez-Santos, email: ivan.perez@ulagos.cl

18
19
20
21
22
23
24
25
26
27
28
29
30
31
32
33



34 Abstract

35 The Puyuhuapi Fjord is an atypical fjord, with two mouths, located in northern
36 Patagonia (44.7° S). One mouth lies to the south, close to the Pacific Ocean, whilst the second
37 connects with the Jacaf Channel to the north where a shallow sill inhibits deep water
38 ventilation contributing to the hypoxic conditions below ~100 m depth. Acoustic Doppler
39 Current Profiler moorings, scientific echo sounder transects, and in-situ abundance
40 measurements were used to study zooplankton assemblages and migration patterns along
41 Puyuhuapi Fjord and Jacaf Channel. The acoustic records and in-situ zooplankton data
42 revealed diel vertical migrations of siphonophores, euphausiids and copepods. A dense layer
43 of zooplankton was observed along Puyuhuapi Fjord between the surface and the top of the
44 hypoxic layer (~100 m), which acted as a physic-chemical barrier to the distribution and
45 migration of the zooplankton. Aggregations of zooplankton and fishes were generally more
46 abundant around the sill in Jacaf Channel than anywhere within Puyuhuapi Fjord. In
47 particular, zooplanktons were distributed throughout the entire water column to ~200 m
48 depth, with no evidence of a hypoxic boundary. Turbulence measurements taken near the sill
49 in the Jacaf Channel indicated high turbulent kinetic energy dissipation rates ($\epsilon \sim 10^{-4} \text{ W kg}^{-1}$)
50 and vertical diapycnal eddy diffusivity ($K_\rho \sim 10^{-2} \text{ m}^2 \text{ s}^{-1}$) values. These elevated vertical
51 mixing ensures that the water column well oxygenated and promotes zooplanktons
52 aggregation. The sill region represents a major topographic contrast between the two fjords,
53 and we suggest that this is an feature for future research on carbon export and fluxes in these
54 fjords.

55
56 **Keywords:** ADCP, Acoustic data, zooplankton, scientific echo sounder, Patagonian fjords.

58 1 Introduction

59 Patagonian fjords extend from 41° S to 56° S latitude, and are typically deep and
60 narrow as a result of their formation during glacial progression. Hydrography is characterized
61 by a two layer vertical structure, consisting of a fresh surface layer in the first ten meters of
62 the water column (resulting from glacial melt) that overlays a subsurface salty layer
63 originating in the Pacific Ocean (Silva and Calvete, 2002; Pérez-Santos et al., 2014). Fjord
64 systems play an important role in primary production and carbon cycling by providing a zone
65 where energy and particulate material are exchanged between land and marine ecosystems



(Gattuso et al., 1998). The principal nutrient (nitrate) is supplied to these fjords by oceanic transport, and particularly through the intrusion of Subantarctic water (SAAW), a water mass that may also transport some species of zooplankton (González et al., 2011).

Zooplankton distribution and abundance in Patagonian fjords and channels has been quantified by Palma (2008), using in-situ collections. A total of 220 plankton samples from a number of depth strata between the surface and ~200 m, allowed the detection of several zooplankton groups (e.g. siphonophores, chaetognaths, cladocerans, copepods and euphausiids) and the description of a north south gradient in the abundance of the major species (Palma, 2008). Additionally, Landaeta et al., (2013) studied the vertical distribution of microzooplankton and fish larvae in Steffen fjords (-47.4° S) in four depth strata (200-50 m, 50-25 m, 25-10 m and 10-0 m depth); copepods were the dominant zooplankton group, with the majority collected in the pycnocline.

Most studies to date in Chilean coastal waters have used various types of plankton nets deployed in a series of depth strata in order to examine the vertical distribution of various zooplankton species. Although this approach provides accurate results, but large-scale surveys of the fjords are limited by the logistics and expense of collecting and processing large numbers of samples. An alternate approach is to use acoustic techniques that provide high resolution data on diurnal vertical migration (DVM) and aggregation patterns of zooplankton in the water column.

ADCP echo intensity (backscatter) signals have demonstrated the potential to quantify vertical and temporal zooplankton distributions. Dense aggregations of krill have been detected and shown to have diel vertical migrations using ADCP moorings located around the Antarctic Peninsula, the Kattegat Channel (Norwegian Sea) and off Funka Bay, Japan (Buchholz et al., 1995; Lee et al., 2004; Zhou and Dorland 2004; Brierley et al., 2006). Most studies have focused on behavior of particular species, but the relationship of this behavior to physical/chemical properties and processes (e.g., temperature, salinity, oxygen and turbulence) remains an important scientific question.

Whilst horizontal aggregations of plankton can occur on a scale of kilometers, there has been considerable recent interest in the study of plankton occurring within thin vertical layers whose scale is very small compared to the depth of the oceans (typical vertical thicknesses between 1-10 meters, but at times <1 m). These vertical and horizontal aggregations of plankton have major implications for reproduction, growth and predation of other marine species (Yamasaki et al., 2002). Also, horizontal advection shear instabilities, water column stratification, turbulence, convective overturns and salt-fingering contribute to



the localization and redistribution of plankton biomass, highlighting the relationship between physical processes and biological life cycles (Timothy et al., 1998). There have been few studies of the relationship between small-scale biophysical processes and plankton distribution along the Chilean coast, especially within the fjord and channel systems (Meerhoff et al., 2014). Using in-situ samples together with CTD profiles Castro et al., (2007) investigated the fine-scale distribution of copepods in the Golfo de Arauco (36.9° S) and showed that distributions were grouped into three layers: one group above the thermocline/oxycline, a second group below, and a third group that migrated across the thermocline. This distinction between groups in the vertical dimension highlighted the range of survival strategies present in these organisms. In a previous study in the same zone, they demonstrated that the vertical distribution and diel vertical migrations patterns changed in *Rhincalanus nasutus* as the organisms develop during the summer season, being the first copepodites stages located around the thermocline while the older copepodites and adults vertically migrated along the entire water column, changing between layers moving in opposite directions (Castro et al., 1993).

The present study has two specific goals. The first is to determine how water column properties and turbulent mixing affect the vertical distributions of zooplankton in a Patagonian Fjord system. The second goal is to determine how the zooplankton distributions in this system respond to ventilation and hypoxic conditions (dissolved oxygen below 2 mL L⁻¹ and ~30 % saturation). To achieve these research goals an Acoustic Doppler Current profiler (ADCP) and a scientific echo sounder were deployed to record zooplankton distribution and aggregation patterns on various temporal and spatial scales. These acoustic measurements were validated using in-situ plankton samples. The physical properties of the water column were measured using microstructure profilers and a Conductivity, Temperature, Depth (CTD) profiler equipped with a Dissolved Oxygen sensor.

2 Study Area

Puyuhuapi Fjord and Jacaf Channel are an atypical example of a Patagonian fjord system; the fjord and channel connect and meet the adjacent ocean via southern and northern mouths (Fig. 1). Seasonal hydrographic measurements along Puyuhuapi Fjord have demonstrated a stratified water column except in late winter when the water column became partially mixed due to reduction of freshwater supply from rivers and glacial melting (Schneider et al., 2014). Hypoxic conditions were detected in Puyuhuapi below 100 m depth



where oxygen concentrations were as low as 1 to 2 mL L⁻¹ (Schneider et al., 2014; Pérez-Santos 2017). The observed oxygen depletion could be caused by the intensive salmon farming in the fjord, limited ventilation due to shallow sills, or the input of low-oxygen Equatorial Subsurface Water into the fjord (Silva and Vargas, 2014).

3 Data and methodology

3.1 Water column properties

Hydrographic surveys were conducted from 1995-2015 in Puyuhuapi Fjord and Jacaf Channel (Fig. 1). These profiles were obtained with a Seabird 25 CTD equipped with a dissolved oxygen sensor and had a vertical resolution of ~12 cm sampling at 8 Hz with a descent rate of ~1 m s⁻¹. The data collected were averaged into one meter bins according to Seabird recommendations. The conservative temperature and absolute salinity (g kg⁻¹) were calculated according to the Thermodynamic Equation of Seawater 2010 (COI et al., 2010). Additionally, nitrate samples were taken using a Niskin bottle at various depths and analyzed spectrophotometrically following the methods of Strickland and Parsons (1968). In-situ dissolved oxygen concentrations were measured to validate oxygen data collected by the oxygen sensor on the CTD. The in-situ oxygen samples were analyzed using the Winkler method (Strickland and Parsons, 1968), which uses a Metrohm burette (Dosimat plus 865) and automatic visual end-point detection (AULOX Measurement System).

Microprofiler measurements were collected using two instruments: The Self Contained Autonomous MicroProfiler (SCAMP) manufactured by Precision Measurement Engineering, Inc. and the Vertical Microstructure Profiler (VMP-250) manufactured by Rockland Scientific, Inc. The SCAMP profiler recorded data at 100 Hz, or ~1 mm vertical resolution with a descending free fall speed of ~10 cm s⁻¹. This instrument is equipped with a fast conductivity sensor (accuracy of ±5% of the full conductivity scale), and a fast temperature response sensor (accuracy of 0.010° C). The vertical gradients of temperature measurements were used to calculate the dissipation rate of turbulent kinetic energy (ε) by applying the Batchelor spectrum (Ruddick and Thompson, 2000; Luketina and Imberger, 2001). The VMP-250 was equipped with two airfoil shear probes and two fast response FP07 thermistors, which allowed for data recording at 512 Hz with a descending free fall speed of ~0.7 m s⁻¹. The micro-shear measurements permitted the calculation of the dissipation rate of turbulent kinetic energy (ε), according to Lueck et al., (2002), Eq. (1),



$$\varepsilon = 7.5\nu \left(\overline{\frac{\partial u}{\partial z}} \right)^2, \quad (1)$$

where, ν is the kinematic viscosity, u is the horizontal velocity, z is the vertical coordinate axis

and therefore $\left(\overline{\frac{\partial u}{\partial z}} \right)^2$ is the shear variance.

Using the values of dissipation rate of turbulent kinetic energy, the diapycnal eddy diffusivity (K_ρ) was calculated. The most used formulation was proposed by Osborn (1980), Eq. (2);

$$K_\rho = \Gamma \frac{\varepsilon}{N^2}, \quad (2)$$

where Γ is the mixing efficiency, generally set to 0.2 (Thorpe 2005), and N is the buoyancy frequency. Shih et al. (2005) noted that when the ratio $\varepsilon / \nu N^2$ is greater than 100, the Eq. (2) results in an overestimation. Therefore, they proposed a new parameterization for this case given by Eq. (3):

$$K_\rho = 2\nu \left(\frac{\varepsilon}{\nu N^2} \right)^{1/2}. \quad (3)$$

More recently, Cuypers et al. (2011) used Eq. (3) when $\varepsilon / \nu N^2 > 100$, Eq. (2) when $7 < \varepsilon / \nu N^2 < 100$, and considered null eddy diffusivity when $\varepsilon / \nu N^2 < 7$. This approach was followed here.

3.2 Acoustic data and analysis

Acoustic measurements were obtained with two 307.7 kHz Teledyne RDI Workhorse Acoustic Doppler Current Profilers (ADCP). The upward mounted ADCPs were moored at depths of ~50 m (ADCP-1) and ~100 m (ADCP-2) in north-central Puyuhuapi Fjord (Fig. 1, same location). These data were collected hourly with a vertical bin size of 1 m, over the periods of austral autumn (ADCP-1: May, 2013) and spring-summer (ADCP-2: November 2013 – January 2014). During the final ADCP-2 mooring deployment along Puyuhuapi Fjord, acoustic data was also collected using the scientific echo-sounder SIMRAD CX34 at 38 kHz. Along-fjord sampling with the echo-sounder was conducted during the daylight and night-time hours of January 22-25, 2014 (black line in Fig. 1). In-situ zooplankton sampling (see section 3.3 for details) was carried out at a fixed station close to the ADCP-1 and 2 positions over a period of 36 hours (Fig. 1) in order to validate both acoustic records. In August 2014,



the scientific echo-sounder experiment was repeated, this time covering the eastern Jacaf Channel, where a shallow sill was detected. A 120 kHz transducer was used in addition to the previous sampling with the 38 kHz transducer, and several day/night transects were completed from Puyuhuapi to the eastern Jacaf Channel with special attention paid to Jacaf sill. The vessel speed during both echo-sounder campaigns was maintained between 8-10 knots.

To study the vertical and horizontal distribution of zooplankton in Puyuhuapi Fjord and Jacaf Channel, the echo intensity from ADCPs was combined with the echoes registered from 38 and 120 kHz with a SIMRAD EK-60 echo-sounder. The zooplankton data registered with the echo-sounder was extracted as the mean volume backscattering strength (Sv) difference between the two measurement frequencies (38 and 120 kHz). Noise from the surface (4 meter) and the bottom was removed from the echoes by using the Echoview software (CITA). After, the Ballon et al., (2011) methodology was applied to all echograms in order to split zooplankton organisms into a “fluid-like” group (i.e, euphausiids, copepods, salps, siphonophores (without gas bladders) and a “blue-like” group that includes fish larvae, gelatinous and gas-bearing and siphonophores. The Sv values obtained with EK-60 echo-sounder were converted into the acoustical nautical area scattering coefficient (NASC, in units of $\text{m}^2 \text{ n mi}^2$, Eq. 4), and used as an index of zooplankton abundance (Ballon et al., 2011), i.e.,

$$NASC = 4\pi(1852)^2 SvT. \quad (4)$$

T was obtained by the integration of cells using 1 m depth in the vertical plane and 10 minutes in the horizontal plane.

The ADCP echo intensity was converted to the mean volume backscattering strength (Sv, dB re 1 m^{-1}), similar to the data recorded by the scientific echo-sounder. The following formula was used for this conversion, Eq. (5):

$$Sv = C + 10\log[(Tx + 273.16)R^2] - L_{DBW} - P_{DBW} + 2\alpha R + K_c(E - E_r) \quad (5)$$

where, C is a sonar-configuration scaling factor (-148.2 dB for the Workhorse Sentinel), T_x is the temperature at the transducer ($^{\circ}\text{C}$), L_{DBW} is $10\log(\text{transmit-pulse length in meters})$. The transmit pulse length was found to be $L=8.13 \text{ m}$. $P_{DBW}=15.5 \text{ W}$ is $10\log(\text{transmit power, in W})$, α is the absorption coefficient (dB m^{-1}), K_c is a beam-specific sensitivity coefficient (supplied by the manufacturer as 0.45), E is the recorded AGC (automatic gain control), and E_r is the minimum AGC recorded (40 dB for ADCP-1 and 41 dB for ADCP-2). The beam-average of the AGC for the 4 transducers was used to obtain optimal results following the procedure in Brierley et al., (2006). Finally, R is the slant range to the sample bin (m), and as



discussed in Lee et al., (2004), which uses the vertical depth as a correction. Therefore, R is obtained with the following equation (6):

$$R = \frac{b + \frac{L+d}{2} + ((n-1)d) + (d/4)}{\cos \zeta} \frac{\bar{c}}{c_l} \quad (6)$$

where b is the blanking distance (3.23 m). The variable L is the transmit pulse length (m), which is the same as $L=8.13$ m in equation 2. The variable d is the length of the depth cell (1 m), n is the depth cell number of the particular scattering layer being measured, ζ is the beam angle (20°), \bar{c} is the average sound speed from the transducer to the depth cell (1453 m s^{-1}) and c_l is the speed of sound used by the instrument (1454 m s^{-1}).

3.3 Zooplankton sampling

In situ zooplankton samples were collected with a WP2 net (60 cm diameter mouth opening, 300 μm mesh, flow meter mounted in the net frame) towed vertically from 50 m to the surface in May 2013, and a Tucker Trawl net using oblique plankton tows (1 m^2 mouth opening, 300 μm mesh with flow meter) in January 2014 and August 2014. All samples were preserved in a 5% formaldehyde solution (Castro et al., 2007). Zooplankton abundances were standardized to individuals per m^3 of filtered seawater (Castro et al., 2007, 2011; Valle-Levinson et al., 2014). The WP2 vertical tows consisted of 5 depth intervals from surface to 50 m, every 10m (0-10, 10-20, 20-30, 30-40, 40-50m). The original sampling design consisted of samplings every 3 hours during a 24h sampling period but, due to a night storm, sampling was reduced to late afternoon and mid-morning and early afternoon sampling of the following day. The stratified zooplankton sampling with the Tucker trawl net (depth strata: 0-10 m, 10-20 m, 20-50 m, 50-100 m, and 100-150 m depth) took place during a 36-h period every 3 h in January 22-24, 2014 (Puyuhuapi Fjord) and every 6 h in August 18-19, 2016 (Jacaf Channel) (Fig. 1, red point).

4. Results

4.1 Hydrographic features

Temperature profiles collected in Puyuhuapi and Jacaf Channels showed similar structure during the winter and summer campaigns (Fig. 2, a-b). The largest temperature gradients were found between the surface and ~ 80 m depth, ranging from 8.5° C to 15° C in 2014. A thin, fresh layer (salinity values varied from 11 to 27 g kg^{-1}) was found in the first



~10 m of the water column below which salinity varied little (27 to ~33 g kg⁻¹), as result of the presence of Subantarctic Water (SAAW) (Fig. 2, c-d). Hypoxic water (dissolved oxygen below 2 mL L⁻¹ and ~30 % saturation) was detected in Puyuhuapi Fjord below 100 m depth, with oxygen concentration between 1-2 mL L⁻¹ (Fig. 2e). Deep water in Jacaf Channel was more ventilated, with dissolved oxygen values above hypoxic conditions throughout the water column (Fig. 2f). Below 50m depth, both regions contained high nitrate concentrations (Fig. 2, g-h). The most recent hydrographic sampling in Puyuhuapi Fjord showed the permanence of hypoxic conditions down to 120 m depth (Fig. 3d). The lowest dissolved oxygen values were detected at the head of the fjord with ~1.5 mL L⁻¹ and 25% of oxygen saturation (Fig. 3d and 3e). The hypoxic layer was located at the position of the ESSW (Fig. 3c).

3.2 ADCP Acoustic data and in-situ zooplankton samples

Data for ADCP backscatter, echo-soundings and in-situ plankton abundance were concurrently collected during three campaigns (May 8-26, 2013, January 22-24, 2014 and August 15-20, 2014) in Puyuhuapi Fjord and Jacaf Channel. The volume backscatter signal obtained from the ADCP-1 deployed at 50 m depth throughout May 2013 showed marked variability from high (-90 to -75 dB re 1 m⁻¹) to low (-115 to -100 dB re 1 m⁻¹) S_v signals (Fig. 4a). High S_v values (<-90 dB re 1 m⁻¹) were recorded during the night hours (~18:00 h to ~07:00 h), while minimum S_v was observed in daytime (~07:00 h to ~18:00 h) suggesting the incorporation of vertically migrating organisms from their deep layers of residence during daytime (below our ADCP mooring depth, 50 m) to the shallower layer at night. In-situ zooplankton sampling was to be conducted during a 24-h cycle in May 25 to 26th, but it was interrupted during the night due to bad weather (Fig. 4b and c). The most abundant zooplankton groups present were Copepods, Siphonophores, Chaetognaths and Jellyfish (Fig. 4c). A marked change in vertical distribution and in total abundance of the zooplankton groups in the water column was observed from the first sampling hour (late afternoon) to the first night sampling time, revealing the start of the nocturnal migration to the surface coincident with a DVM pattern seen in the ADCP-1 backscatter data (Fig. 4b and 4c). After the night storm, while some zooplankton's remained in the shallower layers the following morning (also seen in the backscatter), others vertically migrated downwards and reached deeper layers (below the ADCP-1 mooring depth).

An additional ADCP-2 mooring was positioned deeper at the same location from November 22, 2013 to January 23, 2014, covering the upper ~100 m of the 250 m deep water



290 column (100 m being the technical depth limit of measurement of this instrument). The
291 backscatter time series from this second ADCP deployment also detected a strong DVM
292 pattern by the zooplankton. This was apparent in the S_v signal (reaching -80 dB re 1 m^{-1}),
293 which extended to ~ 100 m depth, e.g., between January 22-24, 2014 (Fig. 5a). During
294 daylight hours, the strongest zooplankton aggregation was observed between 80-100 m depth;
295 this aggregation started to ascend from 18:00 to 21:00 h and by night-time showed a signal
296 close to the surface, before beginning a vertical decent at $\sim 06:00$ h. In-situ stratified sampling
297 of zooplankton was conducted every 3 hrs (0-10 m, 10-20 m, 20-50 m, 50-100 m and 100-150
298 m) to compare to the S_v records (Fig. 4a, black dots).

299
300 The most abundant mesozooplankton groups were Copepods, Euphausiids,
301 Siphonophores, Chaetognaths, Decapods and Jellyfish (Fig. 5, b-e). Copepods, the most
302 abundant taxa, and zooplankton groups with body length larger than 5 mm varied in
303 abundance simultaneously showing the maximum values at night-time and altogether
304 contributed to the DVM pattern seen in the ADCP-2 backscatter data although displaying a
305 time lag of about 2-3 hours (Fig. 5a and 5b). The mean day vs night vertical distribution of the
306 most abundant zooplankton groups (copepods, euphausiids and siphonophores) also showed
307 elevated abundance during night hours close to surface layer (10-20 m) (Fig. 5c-e) and, out of
308 them, euphausiids showed the clearest diel vertical migration pattern with the maximum
309 abundance at the 10-20 m layer at night and at 20-50 during the day hours.

310

311 3.3 Acoustic data from scientific echo sounder

312 The volume backscattering strength (S_v) obtained from the ADCP moorings provided
313 valuable information on zooplankton distribution and migration patterns in the first 100 m of
314 the water column at one specific location (northern zone of Puyuhuapi Fjord in different
315 seasons; Fig. 4 and 5). To complement these data, along-channel variations of zooplankton
316 were studied during the day (January 22nd, 2014) and night (January 24th to 25th, 2014) using a
317 scientific echo sounder SIMRAD (38 kHz). The along-channel transect conducted during day
318 time (from mouth to head; Fig. 6a) demonstrated a uniform distribution of zooplankton along
319 the fjord. In particular, from the mouth to the head of the fjord, S_v values ranged from -110 dB
320 to -80 dB, and zooplankton were mostly located in the first 100 m of the water column,
321 reinforcing the findings of the ADCPs data (Fig. 4, 5 and 6). The maximum observed value of
322 S_v was -77.3 dB, with an average of -89.1 ± 7 dB. At the ADCP-2 mooring location (black dot



in Fig. 6a), high backscatter signal during day time was found between 50-100 m depth, indicating good agreement between both ADCP-2 and echo sounder data (Fig. 4, 5 and 6). Profiles of NASC (Nautical area scattering coefficient) showed high zooplankton abundance between 50-100 m, followed by a secondary abundance at ~200 m depth (Fig. 6b, Center profile). This indicates that some zooplankton species tolerated the low values of dissolved oxygen and crossed the hypoxic layer (below ~120 m depth), but in general, the dense backscattering layer was observed above the hypoxic layer (>120 m depth; Fig. 6). The highest S_v signal for fishes was also typically detected at ~50 m depth during the day, yet was much higher than the zooplankton signal (<-60 dB; Fig. 6c).

A similar transect was repeated during night hours (Fig. 6d-f). In general, the S_v maximum shifted to the surface from 22:00 to 05:00 hours, suggesting an ascending vertical migration of both zooplankton and fishes (Fig. 6d and 6f). In this later case (fishes) a more clear picture of change in vertical distribution can be obtained at comparing the depth of fish aggregations detected by the echo sounder at the end of the first transect at 17.02 h (Fig. 6c) with the depth of fish aggregations at beginning of the backwards transect at 21.57h. At the mouth and center of fjord the NASC profiler indicated an elevated abundance of zooplankton between 10–70 m depth, but at the head, the profiler indicated a similar structure to profiles observed during the day (Fig. 6e). Overall figures 6a and 6d showed that although the water column depth extended to ~300 m, most zooplankton were concentrated above 100 m depth during both day and night time hours. As dissolved oxygen concentrations typically decrease from 2 mL L⁻¹ to 1 mL L⁻¹ below 100 m depth, zooplanktons in Puyuhuapi Fjord appear to prefer water with a higher oxygen concentration (3-7 ml/l). Furthermore, throughout the day and night zooplanktons were more abundant and located deeper in the water column close to the Puyuhuapi Fjord mouth than at the head (Fig. 6 b and 6e).

In August 2014, additional echo sounder transects were carried out along Puyuhuapi Fjord and Jacaf Channel (~35 km length) this time using two frequencies (38 and 120 kHz) that allowed the separation of zooplankton into Fluid like (FL) and Blue noise (BN) groups (Fig. 7a-d). Again, zooplankton distribution in Puyuhuapi Fjord was concentrated in first 100 m of the water column, but at slightly deeper locations (50-100 m) than observed in the first transects during the previous summer campaigns (Fig. 6), possibly due to the bad weather encountered on the sampling day. Maximum zooplankton aggregations were observed in Jacaf Channel around the submarine sill, where high S_v values were recorded (between -60 and -80 dB). In this site zooplankton were found up to ~200 m depth, showing a strong signal



in the echogram for the Blue noise group (Fig. 7b and 7d), with fishes also abundant in the sill region (Fig. 7e and 7f). The length of the Jacaf sill is 6 km and occurs between km 22 to 27 (Fig. 7) with the shallowest point (50 m depth) occurring at ~24 km.

In order to confirm the abundance of zooplankton around the Jacaf sill, continuous acoustics samplings were repeated across the sill. A high abundance of zooplanktons were again observed (Fig. 8), highlighting the presence of two layers of zooplankton: one layer between 100-150 m and the second layer from 200 to 250 m (Fig. 8d). The in-situ plankton sampling detected highest abundance of euphausiids in layer 100-150 m that matched well with the data for the Fluid like group of 120 kHz (Fig. 8c).

3.4 Relationships between acoustic records and water column properties

In order to examine the relationship between zooplankton behavior and environmental variables of the water column, two fixed profiling stations were used to collect continuous acoustic data in Puyuhuapi Fjord (January 23-24, 2014) and Jacaf Channel (August 18-19, 2014) (Fig. 1, red circles). The period of continuous acoustic measurements (38 kHz) extended for 36 hours, with CTD+DO profiles and in-situ zooplankton samples collected every 3 hours.

The relationship between water temperature and elevated S_v values showed a weak correlation during summer ($R^2=0.30$) and winter ($R^2=0.41$) in Puyuhuapi Fjord and Jacaf Channel, despite the seasonal temperature differences. In general, S_v and NASC (not shown) that are both proxies for zooplankton, show a preferred water temperature between 8-10°C (Fig. 9a and 9b). Also, a positive correlation was observed between S_v and salinity ($R^2=0.29$) in Puyuhuapi (Fig. 9c) and Jacaf ($R^2=0.35$) in (Fig. 9d). The major zooplankton aggregations were registered in oceanic water (salinity > 31). In both Puyuhuapi Fjord and Jacaf Channel, the volume backscatter and both dissolved oxygen and oxygen saturation showed highest R^2 values (~0.6) (Fig. 9e-h). In particular, only 20.4% of the total S_v measurements were located in the deep hypoxic layer of Puyuhuapi Fjord, while just 1.2 % was located in the hypoxic layer in Jacaf Channel (Fig. 9e-h), confirming the preference of zooplanktons for oxygenated waters.

3.5 Mixing process

Turbulence profilers and acoustic measurements were obtained at the same fixed stations described before, in order to evaluate the contribution of vertical mixing to the distribution and abundance of zooplankton (Fig. 10). In both systems, S_v records highlighted



patterns of DVM, where most of the red shade area corresponded to the night-time moment (Fig. 10 a-b). Zooplankton aggregation concentrated in the upper 100 meters in Puyuhuapi Fjord (Fig. 10a) and extended from the surface to the bottom in Jacaf Channel (Fig. 10b). The dissipation rate of turbulent kinetic energy (ε) was lower in Puyuhuapi Fjord than in Jacaf Channel throughout the measurement period (Fig. 10c and d). In Puyuhuapi Fjord, elevated S_v signals (>90 dB) were found when ε was between 10^{-10} to 10^{-8} W kg $^{-1}$ (Fig. 10c), but in the Jacaf Channel ε was significant higher than in Puyuhuapi Fjord (10^{-8} to 10^{-4} W kg $^{-1}$) especially in the subsurface layer (~ 10 -50 m depth), owing to the influence of the sill (Fig. 10d). Overall, volume backscatter and ε were much higher in Jacaf Channel than in Puyuhuapi Fjord, indicating that zooplankton abundance could increase in areas with increased turbulent mixing (Fig. 10b and d).

Other turbulence measurements realized before the present study, in November 2013 (Fig. 11a), registered strong shear around the Jacaf sill with high ε values (10^{-7} to 10^{-4} W kg $^{-1}$). The absolute maximum of ε was measured in the Jacaf-Puyuhuapi confluence at ~ 60 m with $\varepsilon = (4.7 \times 10^{-4}$ W kg $^{-1}$), (Fig. 11b). The diapycnal eddy diffusivity (K_ρ) was also high in the same area with values of 10^{-4} to 10^{-2} m 2 s $^{-1}$ (Fig. 11c).

4 Discussion

4.1 Puyuhuapi Fjord

Previous studies have found hypoxic conditions in Puyuhuapi Fjord (Silva and Vargas, 2014; Schneider et al., 2014) and our study supports these findings (Fig. 2 and 3). Hypoxia is known to have a significant impact on plankton distribution and development, hence on the health of the ecosystem as a whole (Ekau et al., 2010). Some species can tolerate hypoxic water, e.g., smaller species, euphausiids and jellyfish can live under 30% oxygen saturation and dissolved oxygen of 1.6 mL L $^{-1}$. Others taxa, such as some copepods and fishes, may be more sensitive to hypoxia and have preference for oxygen saturations of 50-100% and concentrations of 2.6-5.2 mL L $^{-1}$ (Ekau et al., 2010). The sensitivity to tolerate different oxygen concentrations, however, may vary among organisms from different environments. In coastal upwelling zones along Chile, while some copepods seem to be limited to depth ranges with waters well oxygenated, others seem to be well adapted for residence at minimum oxygen depth zones (Castro et al., 2007).

Acoustic data from moored ADCPs and scientific echo sounder transects showed patterns of diel vertical migration by zooplankton in Puyuhuapi Fjord (Fig. 4 and 5), as shown in Reloncaví fjord, Northern Chilean Patagonia (Valle-Levinson et al., 2014). The study in



the Reloncaví fjord by Valle-Levinson et al. (2014) was the first to use ADCP to examine DVM patterns of zooplankton in a Patagonian fjord and found twilight vertical migrations that were dominated by euphausiids and copepods in this fjord, an area where hypoxic conditions were not observed at the time of sampling. In our study, although we did not observe a twilight vertical migration.

In Puyuhuapi Fjord we recorded a dense acoustic scattering layer between the surface and ~120 m depth, with low abundance in the deep hypoxic layers (120-250 m), suggesting some zooplankton occurred also in this deeper layer. Future research will need to understand the relationship of the deep, yet scarce, zooplankton with hypoxia in Puyuhuapi fjord. A similar acoustic experiment was carried out with a 200 kHz echo sounder in Oslofjord, Norway, where hypoxic conditions dominated the water column down to 60 m depth, and no fish or krill were observed in the hypoxic layer (Røstad and Kaartvedt, 2013).

There was a distinct relationship between zooplankton distribution, as measured by the volume backscatter S_v , and dissolved oxygen. In particular, elevated S_v (-90 to -80 dB) coincided with dissolved oxygen concentrations ranging from 2-5 mL L⁻¹ in Puyuhuapi Fjord, and concentrations of 3-6 mL L⁻¹ in Jacaf Channel. In general, DO (and saturation) values of 3.5 mL L⁻¹ (80 % saturation) and 4.5 mL L⁻¹ (70 % saturation) appeared to be the best conditions for zooplankton in Puyuhuapi Fjord and Jacaf Channel, respectively (Fig. 9), and our data coincide with the study of Ekau et al., (2010).

4.2 Jacaf channel sill region

Patagonian fjords and channels cover an area of ~240,000 km² and feature a complex marine topography, including submarine sills and channel constraints (Pantoja et al., 2014; Inall and Gillibrand, 2010). Bernoulli aspiration, internal hydraulic jumps and intense tidal mixing are all processes that can be found near a fjord sill (Farmer and Freeland, 1983; Klymark and Gregg, 2003; Inall and Gillibrand, 2010; Whitney et al., 2014). In particular, at the sill in the Knight Inlet, Canada, which has features similar to Jacaf Channel, turbulent kinetic energy dissipation rates were quantified with an Advanced Microstructure Profiler (AMP) (Klymark and Gregg, 2003). Values of the dissipation rate of turbulent kinetic energy were found to be approximately $\epsilon=10^{-4}$ W kg⁻¹ in the sill vicinity and decreased away from the sill region ($\epsilon=10^{-7} - 10^{-8}$ W kg⁻¹), (Klymark and Gregg, 2003). Our data showed a similar pattern in the Jacaf Channel, with high values of ϵ (10⁻⁴ W kg⁻¹) and K_ρ (10⁻² m² s⁻¹) found near the sill in the subsurface layer (0-50 m) and lower dissipation rates of TKE in Puyuhuapi Fjord (15 km distance; Fig. 1 and 10). The elevated vertical mixing (high K_ρ) in Jacaf Channel



is due to the barotropic tide interacting with the submarine sill (Schneider et al., 2014; Fig. 10 and 11). Similar results of turbulence behavior was obtained in Martínez Channel (Pérez-Santos et al., 2014), central Patagonian, where semidiurnal internal tide dominated the estuarine dynamics (Ross et al., 2014). Here, primary production levels were lower than in Puyuhuapi and Jacaf due to the influence of the Baker river discharge that enhances stratification and introduces suspended solids into the water column (González et al., 2010; Daneri et al., 2012; González et al., 2013).

Studies have shown that turbulence can influence the vertical distribution of zooplankton, and enhance contact with prey and predators (Visser et al., 2009). Theoretical models have shown that predators experience optimal prey consumption when ϵ ranges between 10^{-6} and 10^{-4} W kg^{-1} (Lewis and Pedley, 2001). The acoustic transects conducted along the Jacaf Channel and near its sill during this study (Fig. 7, 8 and 10) (Fig. 10), showed the highest aggregation of zooplankton and fishes close to the sill (within ~ 1 km), which is the area where highest TKE dissipation were observed ($\sim 10^{-4}$ W kg^{-1} ; Fig. 10 and 11). Thin (2-5 m) and thick (10-50 m) shear layers measure directly with the VMP-250 microprofiler contribute to vertical mixing and may enhance exchange between the subsurface rich nutrient layer (Fig. 2) and the photic layer, where phytoplankton is more abundant, as shown in the conceptual model of figure 12.

The measurements collected near Jacaf sill demonstrated the importance of a sill modulating the vertical mixing in Patagonia fjords and also, its influence on the vertical distribution of oxygen, and thereafter on the zooplankton vertical distribution, particularly at both sides of the sill. The elevated accumulation of zooplankton species around the sill indicates that in there might be a significant modification in the export of carbon to the deep fjord water in particular zones of some fjords, and moreover, by its effects on the vertical distribution of dissolved oxygen around these promontories, modifying the quality of the carbon exported to the bottom. Future researches of carbon flux quantification need incorporate sills regions to test this hypothesis, in order to improve the ocean pump assessment in the context of climate change and variability.

A summary of the processes that can contribute to zooplankton vertical distribution and aggregation in the Puyuhuapi Fjord and Jacaf Channel are presented in a conceptual model (Fig. 12). At the Puyuhuapi Fjord, a shallow oxycline around 100 m depth separate the high nutrient and high production layer (Daneri et al., 2012; Montero et al., 2017) from the hypoxic layer below apparently inhibited high concentration of zooplankton at the deepest layer. Above the hypoxic waters, the turbulent mixing values were relatively low favoring the



contact rates among zooplankton predators and their preys and hence favored zooplankton feeding (Visser et al., 2009). In the Jacaf Channel, in turn, the hypoxic layer occurred deeper which should widen the zooplankton depth range of its habitat. However, zooplankton was not deeply distributed but instead aggregated at depth where turbulent mixing was higher increasing this way their potential encounter rates with their preys, particularly around sills.

5 Conclusion

- The hypoxic layer ($<2 \text{ mL L}^{-1}$ and $<30\%$ saturation) was observed below $\sim 100 \text{ m}$ depth along Puyuhuapi Fjord whereas the Jacaf Channel it deeper and thus this fjord was more ventilated owing enhanced the vertical mixing created by the shallow sill .
- Diel vertical migration (DVM) of zooplankton was detected in both the Puyuhuapi Fjord and the Jacaf Channel using ADCP backscatter signal and the scientific echo sounder. However, most of the migrating species in Puyuhuapi Fjord stopped at the hypoxic boundary layer and apparently did not tolerate the hypoxia conditions, situation that was not observed in Jacaf Channel. The most important zooplankton groups detected with in-situ zooplankton net sampling were siphonophores, euphausiids and copepods, being the copepods probably the taxa registered most abundantly in deeper waters and inside the hypoxic layer, coinciding with a scattering signal.
- A dome-shaped correlation as “optimal windows” was demonstrated between oceanographic variables and the relative abundance of zooplankton (dissolved oxygen, $R^2=0.6$, salinity, $R^2=0.3$ and temperature, $R^2=0.35$). This highlighted the preference of zooplankton for well oxygenated water ($3\text{-}6 \text{ mL L}^{-1}$, $60\text{-}80\%$ saturation) with temperatures of $8\text{-}10^\circ\text{C}$, conditions characteristic of SAAW water.
- Scientific echo sounder records showed high aggregation of zooplankton and fishes around the Jacaf sill, where high dissipation rate of turbulent kinetic energy ($\epsilon \sim 10^{-4} \text{ W kg}^{-1}$) and vertical diapycnal eddy diffusivity ($K_\rho \sim 10^{-2} \text{ m}^2 \text{ s}^{-1}$) were recorded with microprofiler instruments. Turbulence appears to be the oceanographic process that contributes to the vertical mixing in the Jacaf channel, helping to the interchange of nutrient, feeding, prey-predator relationship and to the carbon export.



525 **Acknowledgment**

526 The ADCP data was collected as part of the FONDECYT Grant 3120038 by Dr. Iván Pérez-
527 Santos and the help of Dr. Wolfgang Schneider's research group. We thank Dr. Luis Cubillos
528 and Dr Billy Ernst for providing the scientific echo sounder and Cristian Parra and Hernán
529 Rebolledo for the scientific echo sounder sampling. COPAS Sur-Austral CONICYT PIA
530 PFB31 financed part of the field work, and Lauren Ross and Arnoldo Valle-Levinson's trips
531 to Patagonia. We thank Juan Ramón Velasquez for his assistance in the ADCP mooring and
532 Adolfo Mesa, Aldo Balba and Eduardo Escalona for conducting most of the zooplankton
533 sampling. Iván Pérez-Santos was supported by the FONDECYT Grants 11140161 and
534 Giovanni Daneri is funded by FONDECYT Grant 1131063.

535

536 **References**

- 537 Brierle A., Saunders R. A., Bone D. G., Murphy E. J., Enderlein P., Conti S. G., Demer D. A.:
538 Use of moored acoustic instruments to measure short-term variability in abundance of
539 Antarctic krill, *Limnol. Oceanogr.*: Methods 4,18–29, 2004.
- 540 Castro, L.R., Bernal, P.A., Troncoso, V.A.: Coastal intrusion of copepods: mechanisms and
541 consequences in the population biology of *Rhincalanus nasutus*. *J. Plankton Res.* 15
542 (5), 501–515, 1993.
- 543 Castro L.R., M.A. Caceres, N. Silva, M.I. Muñoz, R. León, M.F. Landaeta, Soto Mendoza S.:
544 Short-term variations in mesozooplankton, ichthyoplankton, and nutrients associated
545 with semi-diurnal tides in a Patagonian Gulf, *Con. Shelf Res.*, Vol. 31, 3–4, 282–292,
546 2011.
- 547 Castro L. R., Troncoso V. A.: Fine-scale vertical distribution of coastal and offshore copepods
548 in the Golfo de Arauco, central Chile, during the upwelling season, *Prog. Oceanogr.*
549 75(3): 486–500, 2007.
- 550 Daneri, G., Montero P., Lizárraga L., Torres R., Iriarte J.L., Jacob B., González H.E. and
551 Tapia F.J.: Primary productivity and heterotrophic activity in an enclosed marine area
552 of central Patagonia (Puyuhuapi channel; 44S, 73W). *Biogeosciences Discuss* 9,
553 5929–5968, 2012.
- 554 Ekau W., Auel H., Portner H.-O. and Gilbert D.: Impacts of hypoxia on the structure and
555 processes in pelagic communities (zooplankton, macro-invertebrates and fish).
556 *Biogeosciences*, 7, 1669–1699, 2010.



- 557 Farmer, D. M. and Freeland, H. J.: The physical oceanography of fjords, *Prog. Oceanogr.*, 12,
558 147–194, 1983.
- 559 Gattuso. J., Frankignoulle M., Wollast R.: Carbon and carbonate metabolism in coastal
560 aquatic ecosystems, *Annu. Rev. Ecol. Syst.* 29: 405-434, 1998.
- 561 González, H. E., Calderon, M. J., Castro, L., Clement, A., Cuevas, L. A., Daneri, G., Iriarte, J.
562 30 L., Lizárraga, L., Martinez, R., Menschel, E., Silva, N., Carrasco, C., Valenzuela,
563 C., Vargas, C. A., and Molinet, C.: Primary Production and plankton dynamics in the
564 Reloncavi Fjord and the Interior Sea of Chiloe, Northern Patagonia, Chile, *Mar. Ecol.*
565 *Prog. Ser.*, 402, 13–30, 2010.
- 566 González, H.E., Castro L., Daneri G., Iriarte J.L., Silva N., Vargas C., Giesecke R., Sánchez
567 N.: Seasonal plankton variability in Chilean Patagonia Fjords: carbon flow through the
568 pelagic foodweb of the Aysen Fjord and plankton dynamics in the Moraleda Channel
569 basin, *Cont Shelf Res* 31,225-243, 2011.
- 570 González H. E., Castro L.R., Daneri G., Iriarte J.L., Silva N., Tapia F., Teca E. and Vargas
571 C.A.: Land-ocean gradient in haline stratification and its effects on plankton dynamics
572 and trophic carbon fluxes in Chilean Patagonian fjords (47° – 50°S), *Prog. Oceanogr.*
573 119: 32-47, 2013.
- 574 Greene C.H. and Peter H.W.: Bioacoustical oceanography: New tools for zooplankton and
575 micronekton research in the 1990s, *Oceanography*, 3, 12-17, 1990.
- 576 Inall, M. E. and Gillibrand, P. A.: The physics of mid-latitude fjords: a review, *Geological*
577 *Society, London, UK, Special Publications* 344, 17–33, 2010.
- 578 klymak, J., and Gregg M.: Tidally generated turbulence over the Knight Inlet sill, *J. Phys.*
579 *Oceanogr.*, 34, 1135-1151, 2003.
- 580 Luketina D. A. and Imberger J.: Determining Turbulent Kinetic Energy Dissipation from
581 Batchelor Curve Fitting, *J. Atmos. Oceanic Technol.*, 18, 100–113, doi: 10.1175/1520-
582 0426, 2001.
- 583 Lee, K., Mukai T., Kang D., Iida K.: Application of acoustic Doppler current profiler
584 combined with a scientific echo sounder for krill *Euphausia pacifica* density
585 estimation, *Fisheries Science*, 70: 1051–1060, 2004.
- 586 Lee K., Mukai T., Lee D., Iida K.: Verification of mean volume backscattering strength
587 obtained from acoustic Doppler current profiler by using sound scattering layer,
588 *Fisheries Science*, 74: 221–229, 2008.
- 589 Lewis, D., and Pedley, T.: The Influence of Turbulence on Plankton Predation Strategies, *J.*
590 *theor. Biol.* 210, 347-365, 2001.



- 591 Meerhoff, E., Castro L. and Tapia F.: Influence of freshwater discharges and tides on the
592 abundance and distribution of larval and juvenile *Munida gregaria* in the Baker river
593 estuary, Chilean Patagonia, *Cont. Shelf. Res.* 61–62, 1–11, 2013.
- 594 Montero, P., Pérez-Santos I., Daneri G., Gutiérrez M., Igor G., Seguel R., Crawford D.,
595 Duncan P.: A winter dinoflagellate bloom drives high rates of primary production in a
596 Patagonian fjord ecosystem, *Estuar. Coast. Shelf Sci.*, 199, 105–116, 2017.
- 597 Pantoja, S., Iriarte L., and Daneri, G.: Oceanography of the Chilean Patagonia, *Cont. Shelf*
598 *Res.*, 31, 149–153, 2011.
- 599 Pérez-Santos I., Garcés-Vargas J., Schneider W., Ross L., Parra S., Valle-Levinson A.:
600 Double-diffusive layering and mixing in Patagonia fjords, *Prog. Oceanogr.*, 129, 35–
601 49, 2014.
- 602 Ross, L., Pérez-Santos I., Valle-Levinson A.: Semidiurnal internal tides in a Patagonian fjord,
603 *Prog. Oceanogr.*, 129, Part A, 19–34, 2014.
- 604 Røstad, A. and Kaartvedt S.: Seasonal and diel patterns in sedimentary flux of krill fecal
605 pellets recorded by an echo sounder 1,2 *Limnol. Oceanogr.*, 58 (6), 1985–1997, 2013.
- 606 Ruddick B., A. and Thompson K.: Maximum Likelihood Spectral Fitting: The Batchelor
607 Spectrum, *J. Atmos. Oceanic Technol.*, 17, 1541–1555, doi: 10.1175/1520-0426,
608 2000.
- 609 Schneider, W., Pérez-Santos I., Ross L., Bravo L., Seguel R., Hernández F.: On the
610 hydrography of Puyuhuapi Channel, Chilean Patagonia, *Prog. Oceanogr.*, 128, 8–18,
611 2014.
- 612 Silva, N. and Vargas, C.: Hypoxia in Chilean Patagonia fjords, *Prog. Oceanogr.*, 129, 62–74,
613 2014.
- 614 Sievers, A.H. and Silva, N.: Water masses and circulation in austral Chilean channels and
615 fjords, in: Silva, N., Palma, S. (Eds.), *Progress in the oceanographic knowledge of*
616 *Chilean inner waters, from Puerto Montt to Cape Horn. Comité Oceanográfico*
617 *Nacional - Pontificia Universidad Católica de Valparaíso, Valparaíso, Chile*, pp. 53–
618 58. Book on line at <http://www.cona.cl/>, 2008.
- 619 Strickland, J.D.H. and Parsons, T.R.: A Practical Handbook of Seawater Analysis. *Bull. Fish.*
620 *Res. Board Can.* 167, 1968
- 621 Valle-Levinson A., Castro L., Cáceres M., Pizarro O.: Twilight vertical migrations of
622 zooplankton in a Chilean fjord, *Prog. Oceanogr.* 129, 114–124, 2014.
- 623 Visser, A., Mariani P., Pigolotti S.: Swimming in turbulence: zooplankton fitness in terms of
624 foraging efficiency and predation risk, *J Plankton Res.*, 31 (2): 121–133, 2009



Whitney M., Jia Y., Pearse M., Christopher J. K.: Sill effects on physical dynamics in eastern Long Island Sound. *Ocean Dynamics*, 64:443–458, 2017.

Figure captions

Figure 1. Study area in relation to South America and the Pacific Ocean. The panel to the right enlarges the study area in Puyuhuapi Fjord and Jacaf Channel and indicates the positions of the ADCP-1 and ADCP-2 mooring, the CTD station and acoustic sampling transects, and VMP-250 profiles.

Figure 2. (Upper panel) Profiles of temperature, salinity, dissolved oxygen and dissolved nitrate collected during different oceanographic campaigns in the northern central part of Puyuhuapi Fjord and (lower panel) in eastern region of the Jacaf Channel. The red cross in the oxygen subplot of Jacaf Channel represented the concentration of dissolved oxygen in a discrete in-situ sample, analyzed with Winkler method in order to validate the CTDO data.

Figure 3. Hydrographic measurements undertaken in Puyuhuapi Fjord. (a) Map of the study area showing the transect conducted on June 16 2016 (b) Conservative temperature, (c) absolute salinity, (d) dissolved oxygen and (e) oxygen saturation. Black lines denote sampling profiles. Explain what the acronyms are for the different water masses. Point out the hypoxic layer (dissolved oxygen below 2 mL L⁻¹ and ~30 % saturation). Also state that the x-axis is latitude.

Figure 4. (a) Volume backscattering strength (S_v , dB) calculated from the ADCP-1 backscatter signal in Puyuhuapi Fjord, deployed at 50 m depth from the 8th to the 26th of May, 2013. (b) Zoom of the S_v data and the times of *in situ* zooplankton sampling (black dots) carried out in the AFIOBIOEX I experiment (May 25-26, 2013). (c) Abundance of main zooplankton groups (integrated through the water column to 50 m depth) at the sampling hours indicated in (b).

Figure 5. (a) Volume backscattering strength (S_v , dB) calculated from the ADCP-2 backscatter signal carried out in the AFIOBIOEX II experiment in Puyuhuapi Fjord from the 22nd to the 24th of January, 2014. The *in situ* zooplankton sampling hours are represented by black dots in the top panel. (b) Depth integrated abundance of zooplankton from surface to 150 m depth and (c-e) by depth strata (mean and standard deviation) during day (red) and night (black) of the principal zooplankton groups.

Figure 6. Along-fjord transect using a scientific echo sounder SIMRAD with 38 kHz frequency. Distribution indicated by colors representing S_v . (a-c) Day transect carried out in



658 Puyuhuapi Fjord from the mouth to the head fjord during January 22, 2014. (d-f). Night
659 transect carried out from the head to the mouth fjord, starting at 21:57 January 24th through
660 early in the morning of January 25, 2014. The ADCP-2 mooring location is marked with a
661 black dot. (b-e) Profilers from the Nautical area scattering coefficient (NASC) to the mouth,
662 center and head area of Puyuhuapi Fjord.

663 Figure 7. (a) Scientific echo sounder transects along Puyuhuapi Fjord and Jacaf Channel
664 during August 17, 2014. The left panels (a, b, e) showed the zooplankton and fish distribution
665 with 38 KHz and the right panels (c, d, f) with 120 kHz. Distribution indicated by colors
666 representing Sv. The black dots in a) and c) represented the entrance to Jacaf Channel.

667 Figure 8. (a) Transect along Jacaf sill using the scientific echo sounder during August 18,
668 2014. The left panels (a, b, e) showed the zooplankton and fish distribution with 38 KHz and
669 the right panels (c, d, f) with 120 kHz. Distribution indicated by colors representing Sv.

670 Figure 9. Relationships with the relative abundance of zooplankton expressed in Sv values
671 with the oceanographic variables parameters (a, c, e, g) from Puyuhuapi Fjord and (b, d, f, h)
672 Jacaf Channel.

673 Figure 10. Acoustic and turbulence measurements at fixed stations from Puyuhuapi Fjord and
674 Jacaf Channel. (a-b) Volume backscattering strength, (c-d) Dissipation rate of turbulent
675 kinetic energy with diapycnal eddy diffusivity (contour black lines). (e-f) Scatter plot between
676 the volume backscattering strength and the dissipation rate of turbulent kinetic energy.

677 Figure 11. (a) Microprofilers recorded along Jacaf Channel and sill using VMP-250. (b) The
678 color bar showed the dissipation rate of turbulent kinetic energy values and the blue lines the
679 shear probe results. The horizontal scale (-2 to 2 s^{-1}) applied to profiles 160, 162 and 163. (c)
680 The diapycnal eddy diffusivity profiles, obtained during November 2013.

681 Figure 12. Conceptual model to show the oceanographic process that contribute to the
682 distribution and aggregation of zooplankton in Puyuhuapi Fjord and Jacaf Channel.

683

684

685

686

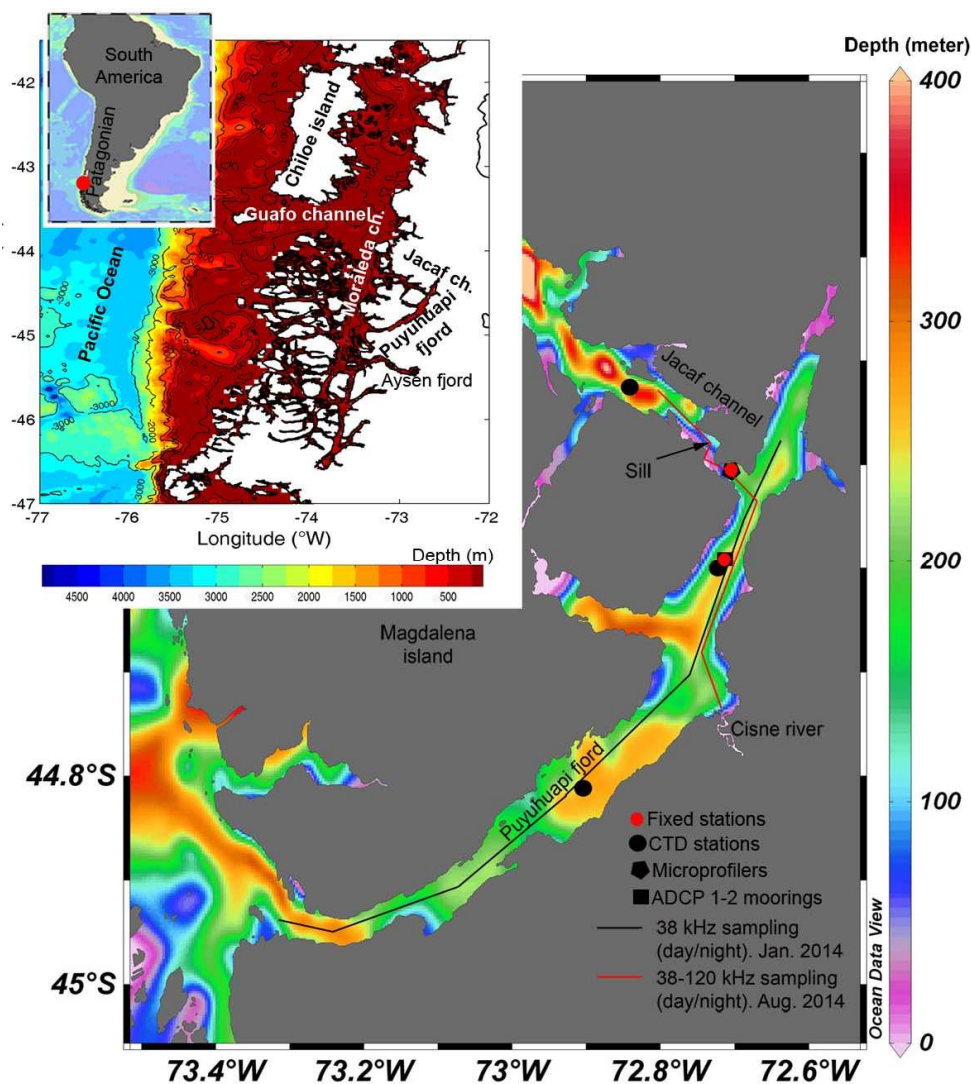


Figure 1. Study area in relation to South America and the Pacific Ocean. The panel to the right enlarges the study area in Puyuhuapi Fjord and Jacaf Channel and indicates the positions of the ADCP-1 and ADCP-2 mooring, the CTD station and acoustic sampling transects, and VMP-250 profiles.

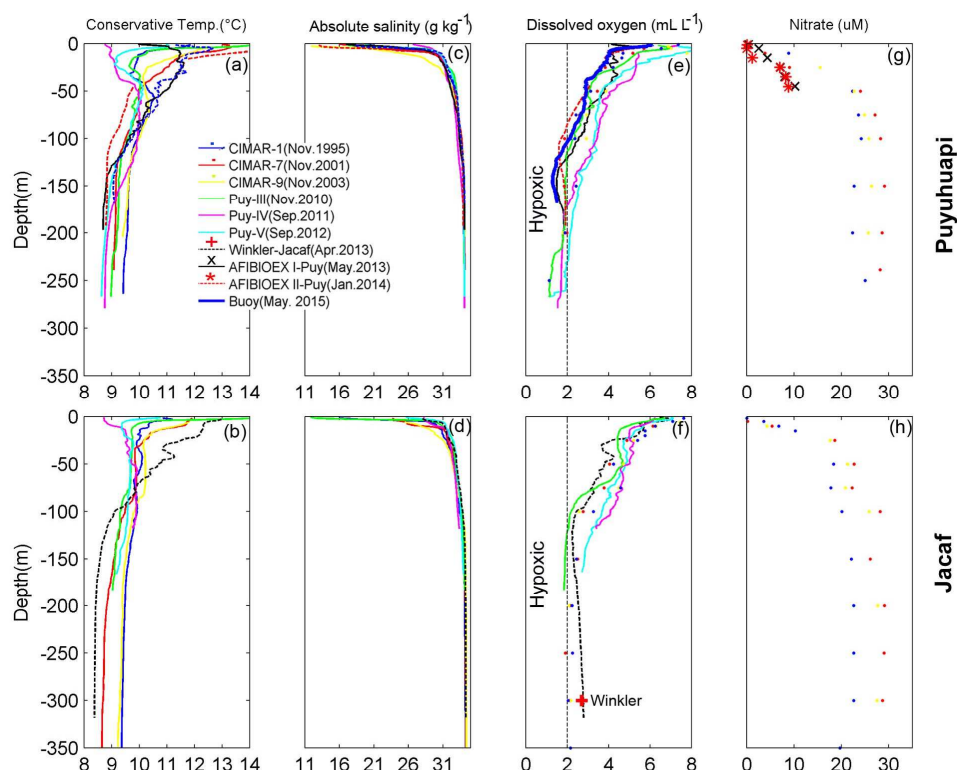
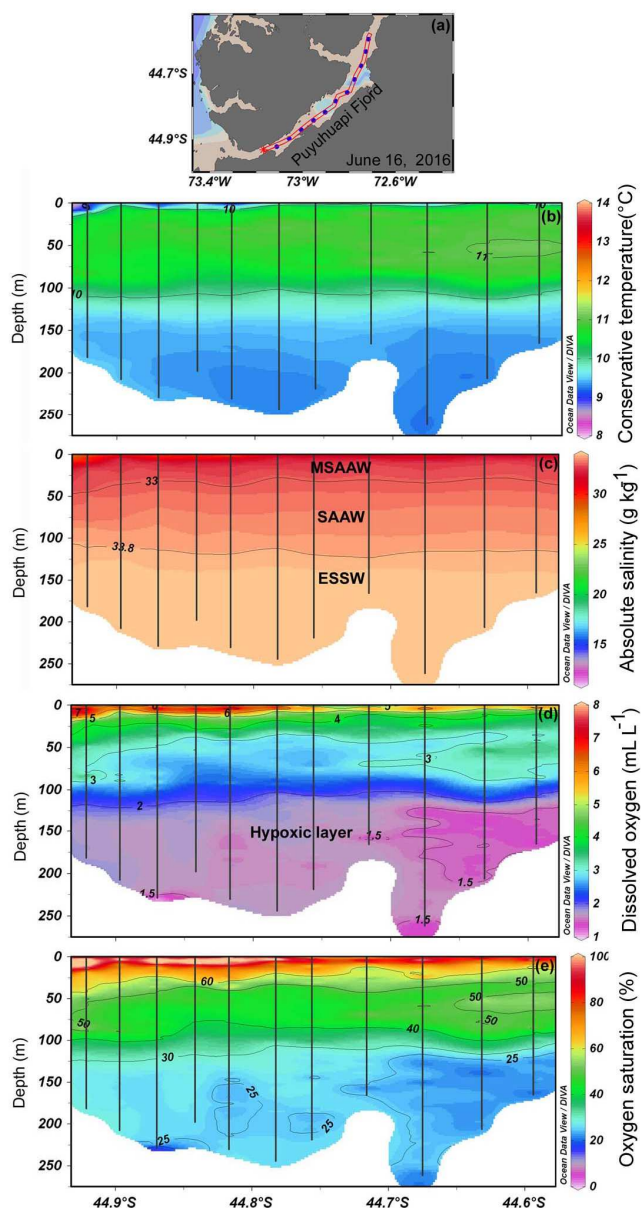
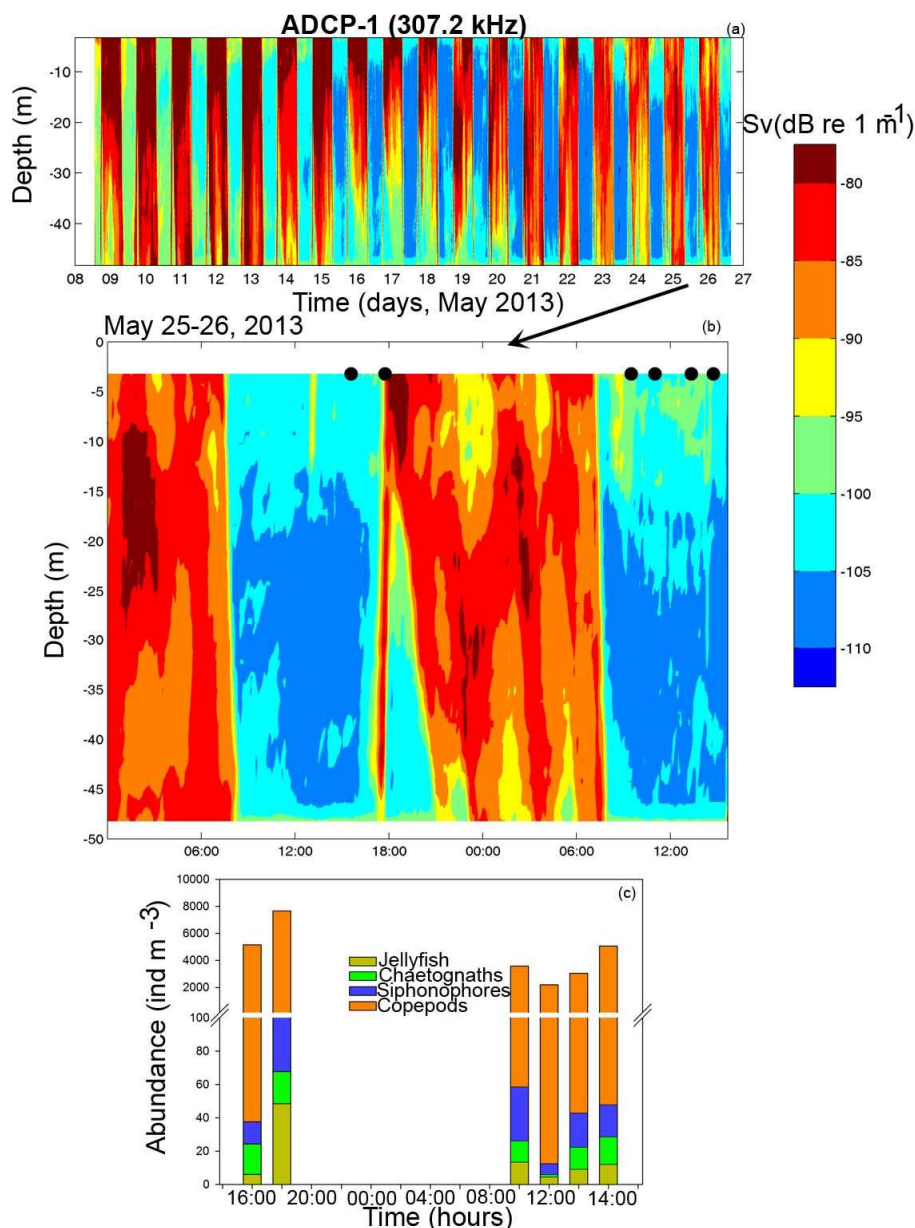


Figure 2. (Upper panel) Profiles of temperature, salinity, dissolved oxygen and dissolved nitrate collected during different oceanographic campaigns in the northern central part of Puyuhuapi Fjord and (lower panel) in eastern region of the Jacaf Channel. The red cross in the oxygen subplot of Jacaf Channel represented the concentration of dissolved oxygen in a discrete in-situ sample, analyzed with Winkler method in order to validate the CTDO data.



706
 707 Figure 3. Hydrographic measurements undertaken in Puyuhuapi Fjord. (a) Map of the study
 708 area showing the transect conducted on June 16 2016 (b) Conservative temperature, (c)
 709 absolute salinity, (d) dissolved oxygen and (e) oxygen saturation. Black lines denote sampling
 710 profiles. Explain what the acronyms are for the different water masses. Point out the hypoxic
 711 layer (dissolved oxygen below 2 mL L^{-1} and $\sim 30 \%$ saturation). Also state that the x-axis is
 712 latitude.



713

714 Figure 4. (a) Volume backscattering strength (S_v , dB) calculated from the ADCP-1 backscatter
 715 signal in Puyuhuapi Fjord, deployed at 50 m depth from the 8th to the 26th of May, 2013. (b)
 716 Zoom of the S_v data and the times of *in situ* zooplankton sampling (black dots) carried out in
 717 the AFIOBIOEX I experiment (May 25-26, 2013). (c) Abundance of main zooplankton
 718 groups (integrated through the water column to 50 m depth) at the sampling hours indicated in
 719 (b).

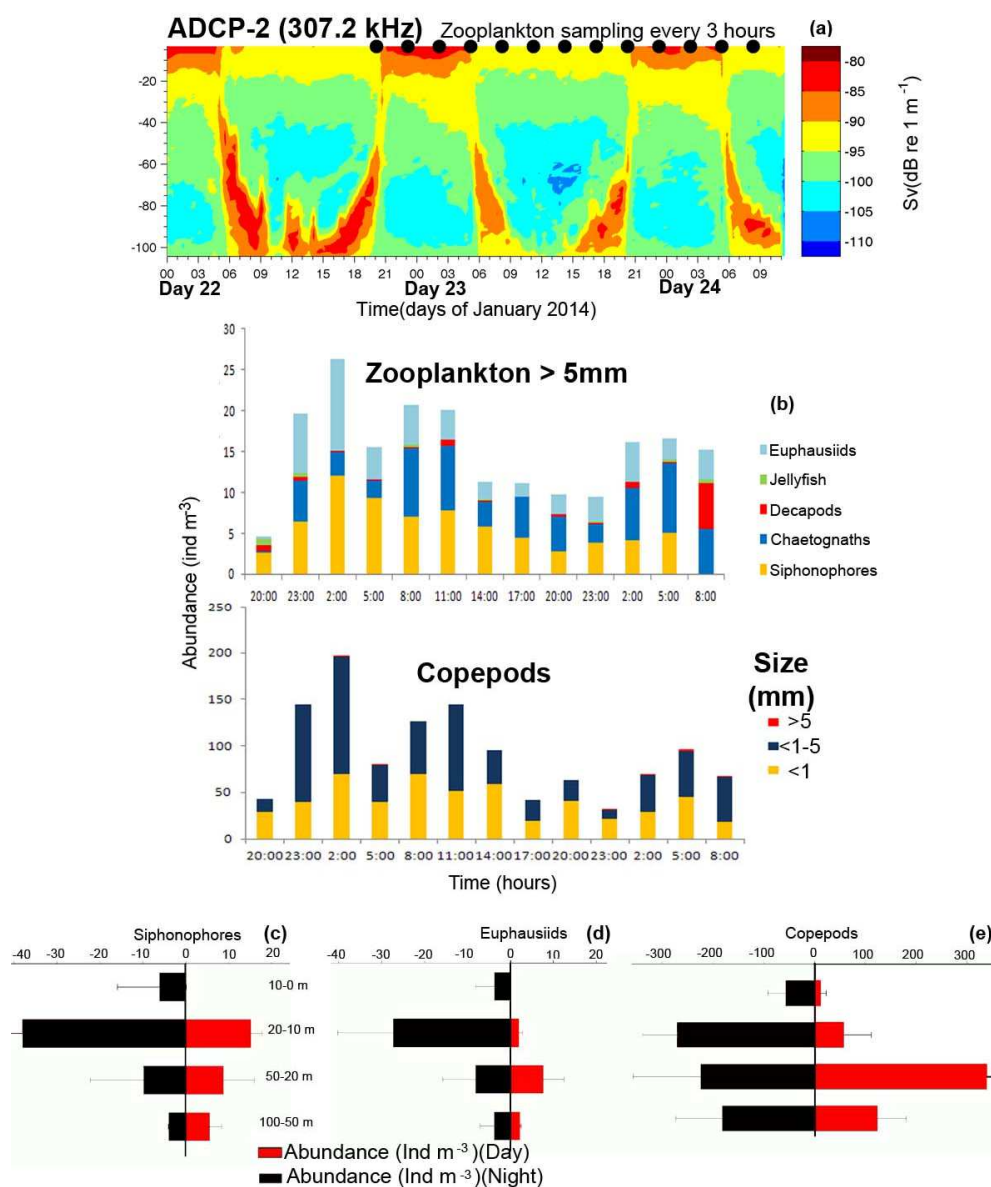
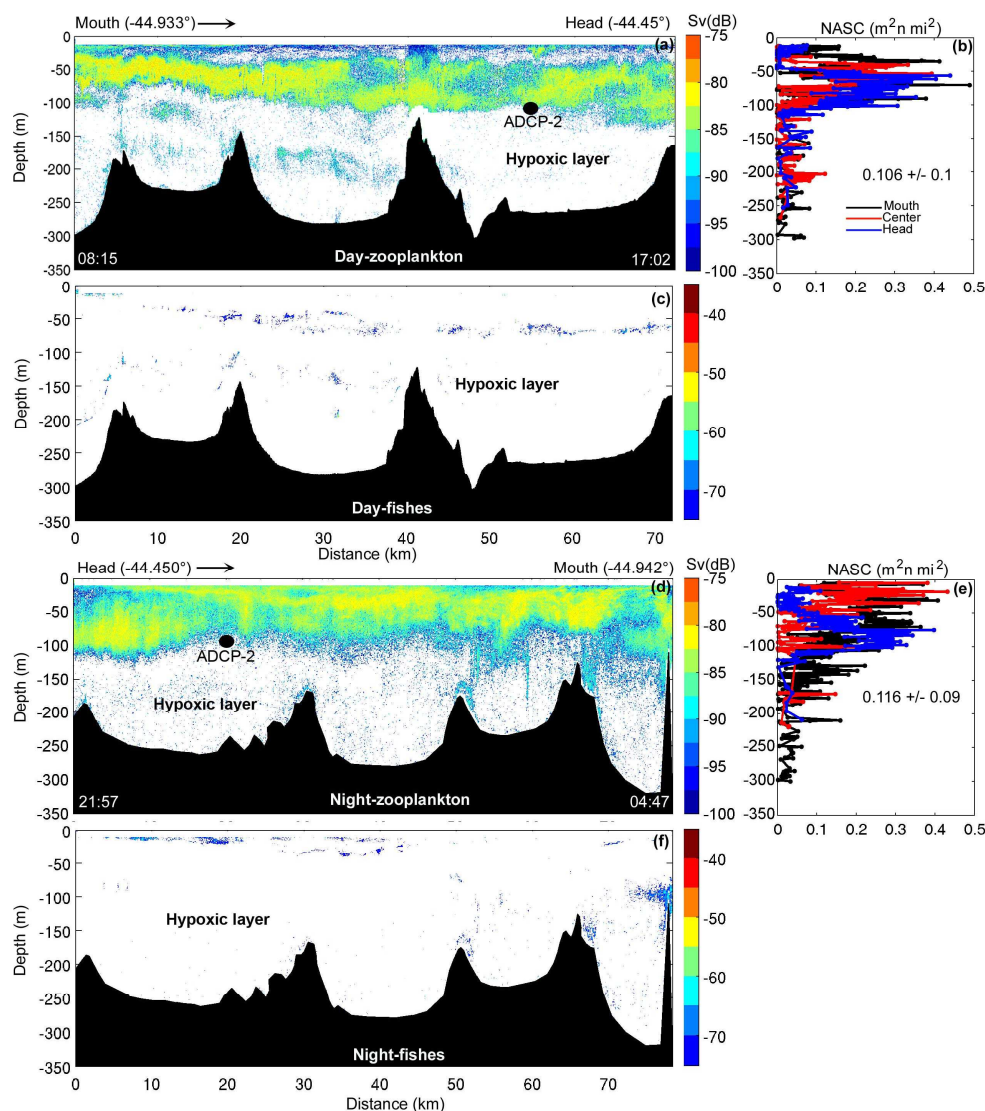
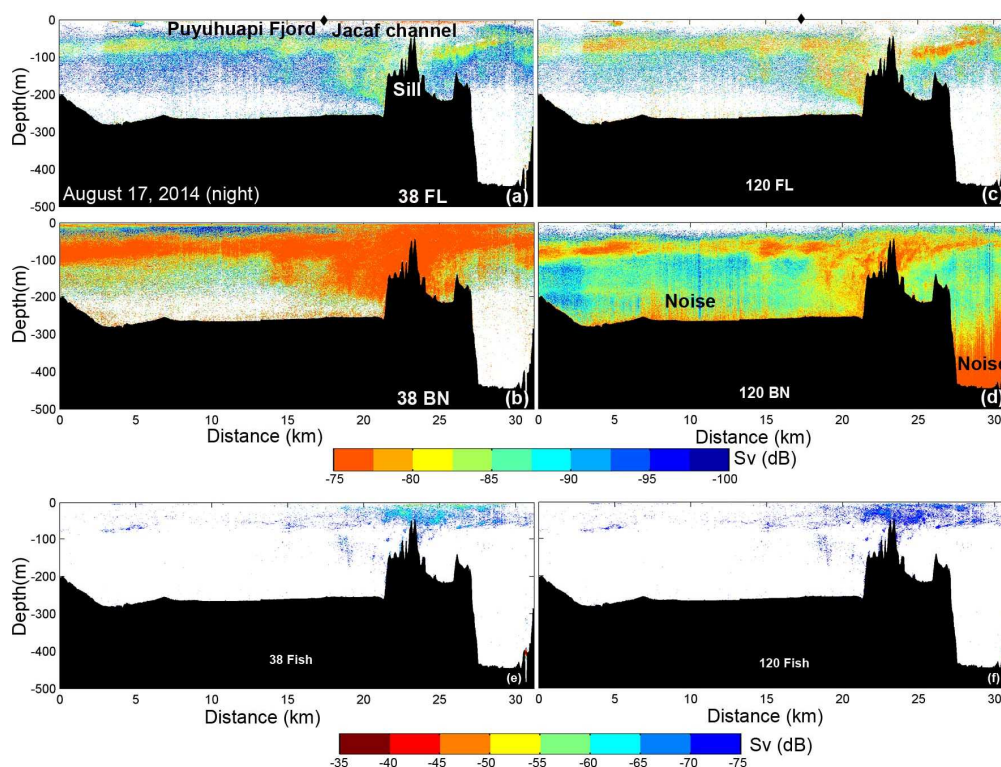


Figure 5. (a) Volume backscattering strength (S_v , dB) calculated from the ADCP-2 backscatter signal carried out in the AFIOBIOEX II experiment in Puyuhuapi Fjord from the 22nd to the 24th of January, 2014. The in situ zooplankton sampling hours are represented by black dots in the top panel. (b) Depth integrated abundance of zooplankton from surface to 150 m depth and (c-e) by depth strata (mean and standard deviation) during day (red) and night (black) of the principal zooplanktons groups.



727
 728 Figure 6. Along-fjord transect using a scientific echo sounder SIMRAD with 38 kHz
 729 frequency. Distribution indicated by colors representing Sv. (a-c) Day transect carried out in
 730 Puyuhuapi Fjord from the mouth to the head fjord during January 22, 2014. (d-f). Night
 731 transect carried out from the head to the mouth fjord, starting at 21:57 January 24th through
 732 early in the morning of January 25, 2014. The ADCP-2 mooring location is marked with a
 733 black dot. (b-e) Profilers from the Nautical area scattering coefficient (NASC) to the mouth,
 734 center and head area of Puyuhuapi Fjord.

735

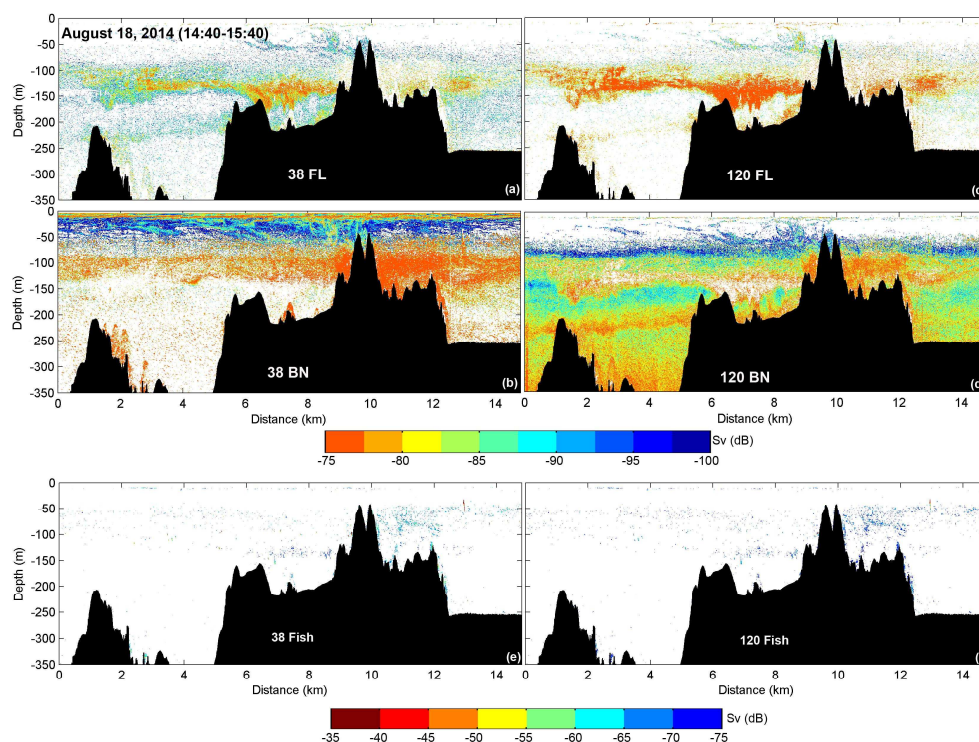


736

737 Figure 7. (a) Scientific echo sounder transects along Puyuhuapi Fjord and Jacaf Channel
 738 during August 17, 2014. The left panels (a, b, e) showed the zooplankton and fish distribution
 739 with 38 KHz and the right panels (c, d, f) with 120 kHz. Distribution indicated by colors
 740 representing Sv. The black dots in a) and c) represented the entrance to Jacaf Channel.

741

742



743

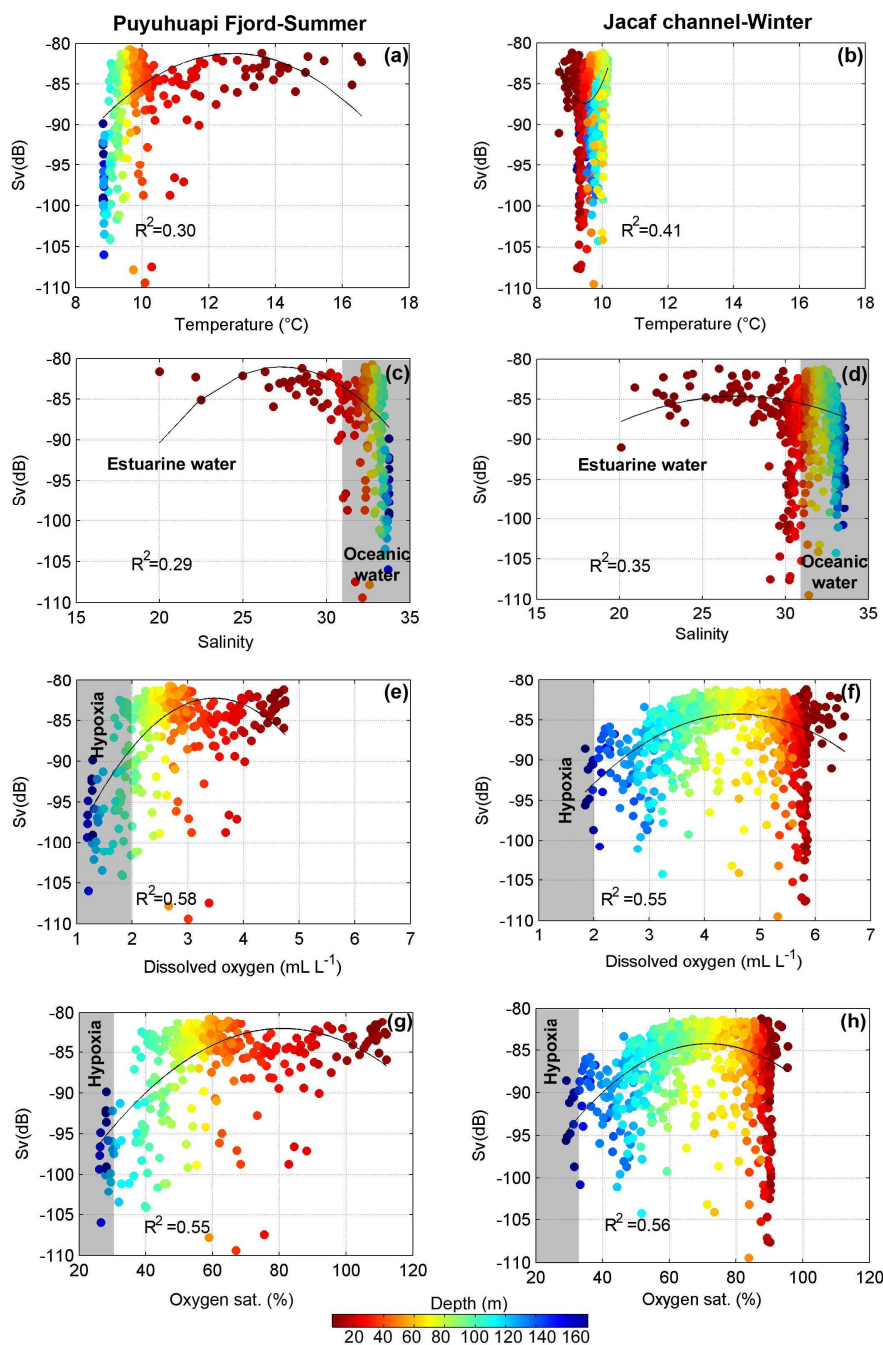
744 Figure 8. (a) Transect along Jacaf sill using the scientific echo sounder during August 18,
 745 2014. The left panels (a, b, e) showed the zooplankton and fish distribution with 38 KHz and
 746 the right panels (c, d, f) with 120 kHz. Distribution indicated by colors representing Sv.

747

748

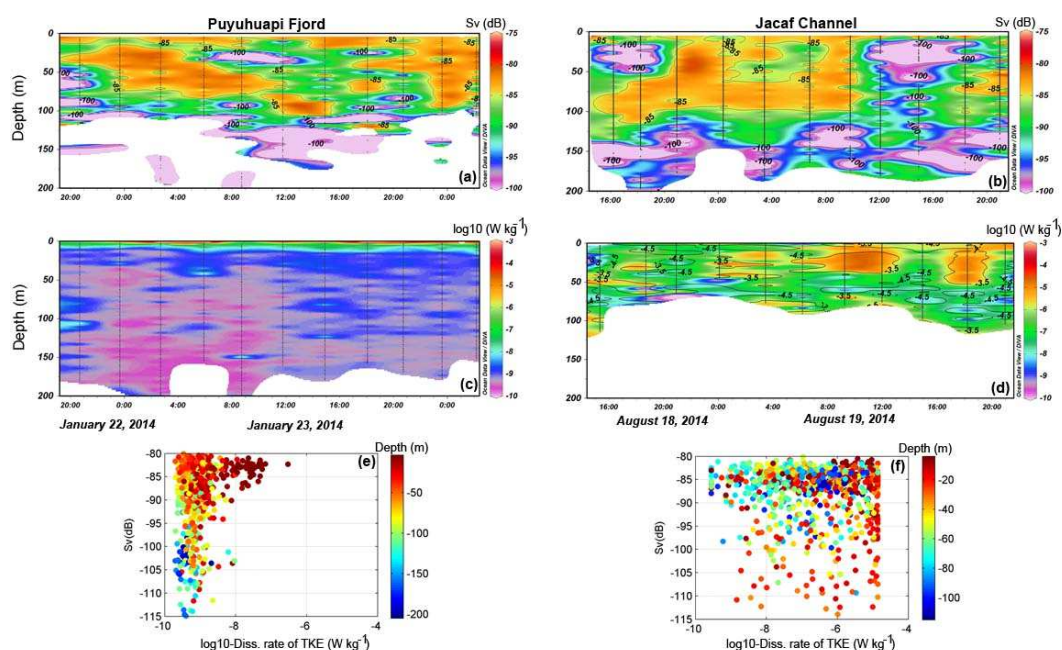
749

750



751

752 Figure 9. Relationships with the relative abundance of zooplankton expressed in Sv values
 753 with the oceanographic variables parameters (a, c, e, g) from Puyuhuapi Fjord and (b, d, f, h)
 754 Jacaf Channel.



755
 756 Figure 10. Acoustic and turbulence measurements at fixed stations from Puyuhuapi Fjord and
 757 Jacaf Channel. (a-b) Volume backscattering strength, (c-d) Dissipation rate of turbulent
 758 kinetic energy with diapycnal eddy diffusivity (contour black lines). (e-f) Scatter plot between
 759 the volume backscattering strength and the dissipation rate of turbulent kinetic energy.

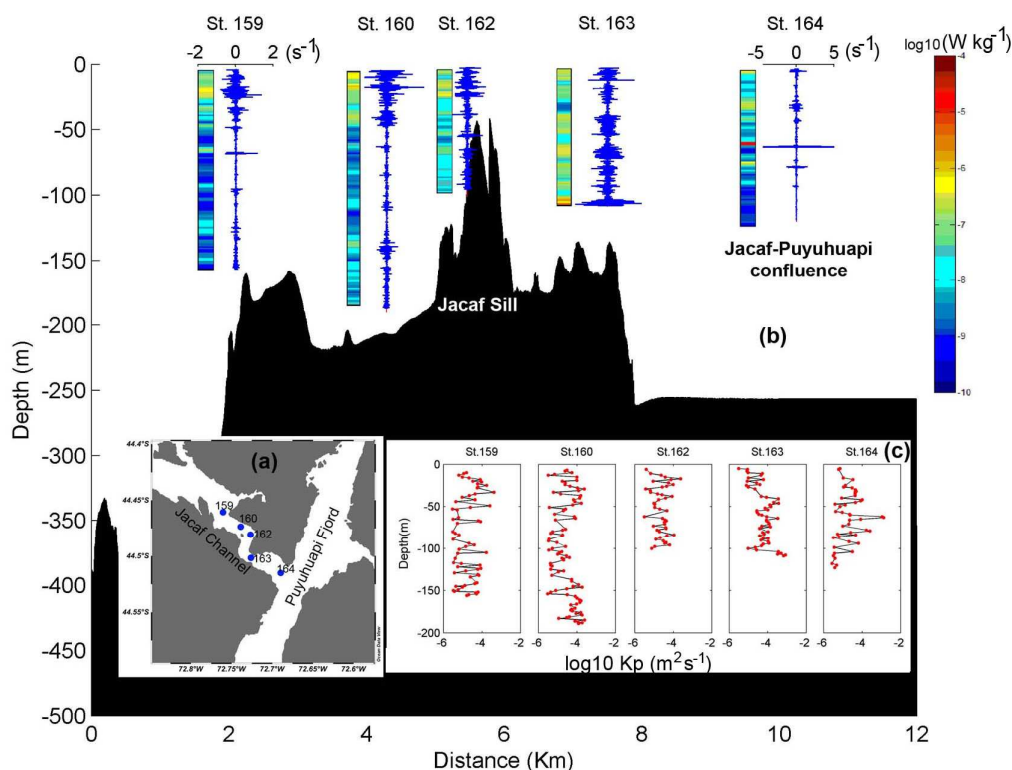
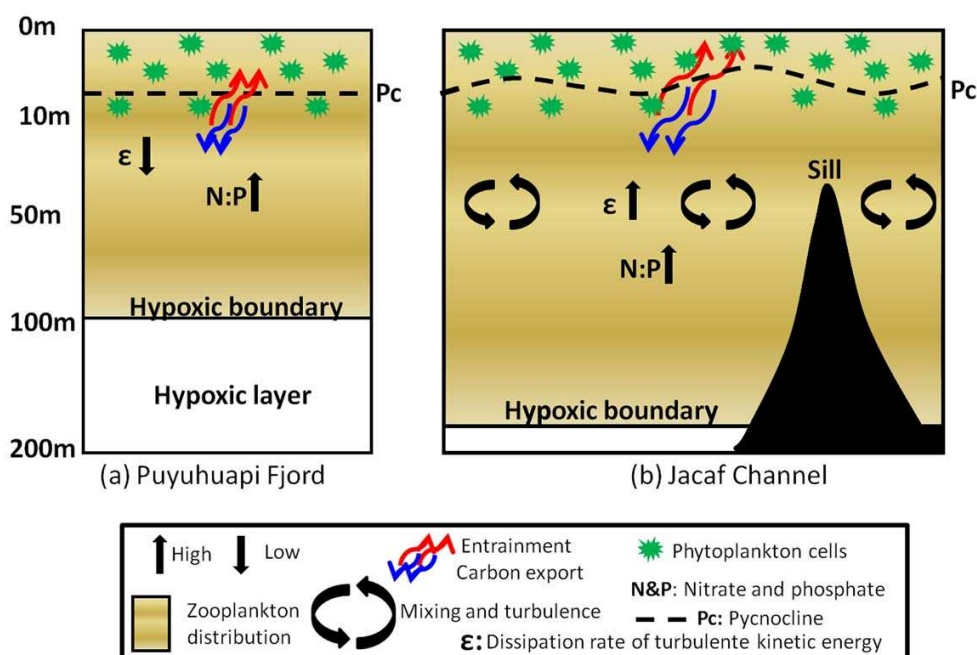


Figure 11. (a) Microprofilers recorded along Jacaf Channel and sill using VMP-250. (b) The color bar showed the dissipation rate of turbulent kinetic energy values and the blue lines the shear probe results. The horizontal scale (-2 to 2 s^{-1}) applied to profiles 160, 162 and 163. (c) The diapycnal eddy diffusivity profiles, obtained during November 2013.



781

782 Figure 12. Conceptual model to show the oceanographic process that contribute to the

783 distribution and aggregation of zooplankton in Puyuhuapi Fjord and Jacaf Channel.